Effects of the near-dipole–dipole interaction on gap solitons in resonantly absorbing gratings

Jing Cheng* and Jianying Zhou†
State Key Laboratory of Optoelectronic Materials and Technologies, Zhongshan University, Guangzhou 510275, People's Republic of China

(Received 17 April 2002; published 18 September 2002)

Gap solitons can exist in a periodic refractive-index grating modified by periodic layers of near-resonant two-level systems. In this work, we include the effect of the density-dependent near-dipole–dipole (NDD) interaction in order to generalize this model. For certain values of the grating parameters, we find that the NDD interaction significantly modifies the frequency bands in which gap solitons can exist. The difference between the model with and without the NDD interaction is discussed. The stability of gap solitons is studied numerically.

DOI: 10.1103/PhysRevE.66.036606 PACS number(s): 42.65.Tg, 42.70.Qs, 42.25.Bs, 42.50.Gy

I. INTRODUCTION

The light-matter interactions in linear or nonlinear photonic band gap (PBG) materials have received much attention [1]. In linear PBG, the Bragg reflections block the propagation of light in certain spectral bands. However, there exists a generic type of solitary wave whose intrinsic frequency belongs to this spectral gap [2,3]. Typically, optical gap solitons are found in models of resonant Bragg gratings equipped with various nonlinearities, including the Kerr nonlinearity [4,5] and second-harmonic generation [6]. Gap solitons have been observed experimentally in a short Kerr-nonlinear glass fiber with a Bragg grating written on it [7].

Recently, a kind of gap solitons (GS) has been found in the resonantly absorbing Bragg reflector (RABR) [3,8–10], which is a periodic array of thin layers of resonant two-level systems (TLS) separated by half-wavelength nonabsorbing dielectric layers. In a RABR, both bright and dark solitons can exist in the spectral gap, and the bright solitons can have arbitrary pulse area. Also, the existence of spatial-temporal GS has been studied in multidimensional resonantly absorbing photonic crystal [11,12]. The model of GS in RABR is based on the Maxwell-Bloch equation. The TLS density is a crucial parameter to determine the properties of GS. If the TLS density is very high, then the near-dipole–dipole (NDD) interaction should be included in the Maxwell-Bloch equation. A generalized Maxwell-Bloch equation has been obtained [13], and the local-field correction (LFC) has been shown to produce many interesting phenomena, such as intrinsic optical bistability [14], propagation effects in nonlinear media [15], ultrafast optical switching [16], enhancement of inversionless gain and refractive index without absorption [17], reduction of the electromagnetically induced transparency [18], enhancement of the spontaneous emission rate in a dielectric [19], modification of the superradiant amplification [20], and coherent and incoherent solitons of self-induced transparency [21]. In this paper, we study the effects of NDD interaction on the existence of gap solitons in the RABR. If the density of the TLS is not very low, the NDD interaction will lead to an inversion-dependent resonance frequency in the Bloch equation. We find that this correction significantly modifies the existence of gap solitons.

II. THEORY

Our model is the RABR introduced in Refs. [3,8–10]. A one-dimensional periodic grating with period d has linear refractive-index distribution $n^2(z)=n_0^2[1+\sum_{m=1}^{\infty}a_m\cos(2mk_cz)]$, where $k_c=\pi/d$. This refractive-index distribution gives rise to band gaps. The central frequency of the fundamental gap is $\omega_c=k_cc/n_0$ and the gap edges are at $\omega_{1,2}=\omega_c(1\pm a_1/4)$. Further, thin TLS layers are doped in this structure at the position $z_j=jd$. The resonance frequency ω_0 of the TLS is close to the gap center ω_c, the transition dipole moment is μ, and the TLS density (averaged over z) is σ.

Considering non-negligible NDD interaction, the propagation of electromagnetic waves $E(z,t)$ in RABR must be described by the Maxwell-Bloch equation with the LFC.

According to Ref. [10], we can write down the Maxwell equation

$$c^2\frac{\partial^2E}{\partial z^2}-n^2(z)\frac{\partial^2E}{\partial t^2}=\frac{\partial^2P_{nl}}{\partial t^2}, \tag{1}$$

and the modified Bloch equation for polarization P and population inversion w,

$$\partial_tP=-i(\omega_0-\omega_c)P+\Omega^{loc}w, \tag{2}$$

$$\partial_tw=-\tfrac{1}{2}(P^*\Omega^{loc}+P\Omega^{loc*}), \tag{3}$$

where the Rabi frequency Ω^{loc} is related to the local field E^{loc} by

$$E^{loc}=\frac{\hbar}{2\mu}(\Omega^{loc}e^{-i\omega_ct}+\Omega^{loc*}e^{i\omega_ct}), \tag{4}$$

and the local field is [20]

$$E^{loc}=E+\tfrac{1}{3}P_{nl}+\tfrac{1}{3}P_l, \tag{5}$$

where the linear polarization is

*Electronic address: stp00cj@student.zsu.edu.cn
†Electronic address: stszjy@zsu.edu.cn

$$P_l = 3\frac{n^2-1}{n^2+2}E^{loc}, \tag{6}$$

and the nonlinear polarization takes the form [10]

$$P_{nl} = -2\pi i\sigma\mu(Pe^{-i\omega_c t} - P^* e^{i\omega_c t}). \tag{7}$$

Like the derivation in Ref. [10], we obtain a set of coupling equations from these equations,

$$\left(\frac{\partial^2}{\partial\tau^2} - \frac{\partial^2}{\partial\zeta^2}\right)\Sigma_+ = 2\frac{\partial}{\partial\tau}P + 2i\eta P - \eta^2\Sigma_+, \tag{8}$$

$$\left(\frac{\partial^2}{\partial\tau^2} - \frac{\partial^2}{\partial\zeta^2}\right)\Sigma_- = -2\frac{\partial}{\partial\zeta}P - \eta^2\Sigma_-, \tag{9}$$

$$\frac{\partial}{\partial\tau}P = w\Sigma_+ - i\delta P - i\epsilon w P, \tag{10}$$

$$\frac{\partial}{\partial\tau}w = -\frac{1}{2}(P^*\Sigma_+ + P\Sigma_+^*), \tag{11}$$

where

$$E = \hbar(\mu\tau_0)^{-1}\frac{3}{n_m^2+2}(\mathrm{Re}[\Sigma_+ e^{-i\omega_c t}]\cos k_c z - \mathrm{Im}[\Sigma_- e^{i\omega_c t}]\sin k_c z). \tag{12}$$

The normalized time τ, propagation distance ζ, and detuning δ are defined as

$$\tau = t/\tau_0, \quad \zeta = (n_0/c\tau_0)z, \quad \delta = (\omega_0 - \omega_c)\tau_0,$$

and

$$\tau_0 = n_0\mu^{-1}\sqrt{3\hbar/[2\pi\omega_c\sigma(n_a^2+2)]} \tag{13}$$

is the characteristic absorption time of the field by the TLS, $n_a^2 = n_0^2(1+\Sigma_{m=1}^{\infty}a_m)$. The normalized modulation strength η can be expressed as

$$\eta = \frac{a_1\omega_c\tau_0}{4}. \tag{14}$$

The NDD interaction is given by the term $-i\epsilon wP$ in Eq. (10) where the normalized coupling strength is

$$\epsilon = \frac{4\pi(n_a^2+2)\mu^2\sigma}{9\hbar}\tau_0. \tag{15}$$

Compared with the equations in Ref. [10], the only difference in our model is the inclusion of the LFC term "$-i\epsilon wP$" in Eq. (10). Since ϵ is proportional to the square root of TLS density $\sqrt{\sigma}$, we will show that this correction will give rise to many results when TLS density is high enough.

From Eqs. (10) and (11), it is easy to get a simple relation between the polarization and the population inversion

$$w = \pm\sqrt{1-|P|^2}. \tag{16}$$

Since at the beginning, the TLS is not inversed, the $-$ sign should be chosen in Eq. (16).

First, we try to obtain the linear dispersion relation of the model. Setting $w=-1$ and $\Sigma_+ = Ae^{i(k\zeta-\omega\tau)}$, $P = Ce^{i(k\zeta-\omega\tau)}$, and linearizing Eqs. (8) and (10), the dispersion relation for the wave number k and frequency ω is

$$(\omega-\delta+\epsilon)[\omega^2-k^2-(2+\eta^2)]+2(\eta-\delta+\epsilon)=0. \tag{17}$$

This equation generates three dispersion curves and two frequency gaps as in Ref. [9]. The difference between Eq. (17) and the dispersion relation in Ref. [9] is that δ is replaced by $\delta-\epsilon$.

Inside these gaps, the standing soliton solutions will be sought in the form

$$\Sigma_+(\zeta,\tau) = e^{-i\chi\tau}s(\zeta), \quad P(\zeta,\tau) = ie^{-i\chi\tau}q(\zeta), \tag{18}$$

with real functions $s(\zeta)$ and $q(\zeta)$. Using Eqs. (10), the inversion w can be expressed as

$$w = \frac{\chi-\delta}{s+\epsilon q}q. \tag{19}$$

Substituting it into Eq. (16), we get

$$s = q\left(-\epsilon - \frac{\chi-\delta}{\sqrt{1-q^2}}\right). \tag{20}$$

From Eq. (8),

$$\frac{d^2s}{d\zeta^2} = (\eta^2-\chi^2)s + 2(\eta-\chi)q. \tag{21}$$

Using Eq. (20), Eq. (21) can be integrated,

$$\frac{1}{2}\left(\frac{dq}{d\zeta}\right)^2\left(-\epsilon - \frac{\chi-\delta}{\sqrt{(1-q^2)^3}}\right)^2 + F(q) = C_0, \tag{22}$$

where

$$F(q) = -\left[\frac{(\eta^2-\chi^2)(\chi-\delta)^2}{2(1-q^2)} + \frac{\epsilon(\eta-\chi)[-2+\epsilon(\chi+\eta)]q^2}{2} + \frac{(\eta-\chi)(\chi-\delta)[-2+\epsilon(\chi+\eta)q^2]}{\sqrt{1-q^2}}\right], \tag{23}$$

and C_0 is the integration constant. Equation (22) can be written as

$$\frac{d^2q}{d\zeta^2} = -\frac{dU(q)}{dq}, \tag{24}$$

$$U(q)=\frac{F(q)-C_0}{\left(-\epsilon-\dfrac{\chi-\delta}{\sqrt{(1-q^2)^3}}\right)^2}, \tag{25}$$

which is similar to Newton's equation of motion for a particle with coordinate $q(\zeta)$ moving in a potential $U(q)$.

If the solution of Eq. (24) is solitonlike, then $q(\pm\infty)=0$. This means that the "particle" begins at time $-\infty$ on position $q=0$, moves to one side, and finally returns back to $q=0$ at time $+\infty$. It is reasonable to require $q'(\pm\infty)=0$, otherwise the solution will be oscillate. From these consideration, the integration constant can be determined, $C_0=F(0)$.

Now, we look for the frequency bands where gap solitons can appear. At $q=0$, $F(q)$ has the Taylor expansion to q^2 term

$$\begin{aligned}F(q)=&\tfrac{1}{2}\{(\chi^2-\eta^2)(\chi-\delta)^2+\epsilon(\chi-\eta)[-2+\epsilon(\chi+\eta)]\\&-2(\chi-\eta)(\chi-\delta)+2(\chi^2-\eta^2)(\chi-\delta)\epsilon\}q^2\\&+O(q^4).\end{aligned} \tag{26}$$

If $F(q=0)=0$ is a local maximum, i.e., $F''(0)<0$, and $F(q)\to\pm\infty$ when $q\to\pm1$, then $U(0)=0$ is the local maximum of $U(q)$ and the global maximum of $U(q)$ is larger than zero, thus Eq. (24) has solitonlike solutions. These conditions require

$$|\chi|>\eta, \tag{27}$$

$$\begin{aligned}&(\chi^2-\eta^2)(\chi-\delta)^2+\epsilon(\chi-\eta)[-2+\epsilon(\chi+\eta)]-2(\chi-\eta)\\&\times(\chi-\delta)+2(\chi^2-\eta^2)(\chi-\delta)\epsilon<0.\end{aligned} \tag{28}$$

The left-hand side of Eq. (28) has four real roots depending on the values of η, ϵ, δ. We specify them by $x_1>x_2>x_3>x_4$, so there are two frequency bands of χ, $x_1>\chi>x_2$ and $x_3>\chi>x_4$ in which Eq. (28) is satisfied. Combining with Eq. (27), we can determine the frequency bands where solitons can exist.

It is possible to have one or two frequency bands for solitons. Typical results are shown in Figs. 1 and 2. In calculation, we set the values of a_1, n_0, ω_0/ω_c, and vary η as an independent parameter. Then δ and ϵ can be expressed by η,

$$\delta=\frac{4}{a_1}\left(\frac{\omega_0}{\omega_c}-1\right)\eta, \tag{29}$$

$$\epsilon=\frac{a_1 n_0^2}{6\eta}. \tag{30}$$

Using Eqs. (13), (14), (29), and (30), only the TLS density remains as a free parameter. So we can study the effects of NDD interaction on the existence of gap solitons.

In Fig. 1(a), $a_1=0.2$, $n_0=3.5$, $\omega_0/\omega_c-1=-0.03$, the roots of Eq. (28) are plotted as a function of η. Also $\chi=-\eta$ is plotted. From this figure, we can see if $\eta<0.608$, there are two frequency bands filled with solitons. If

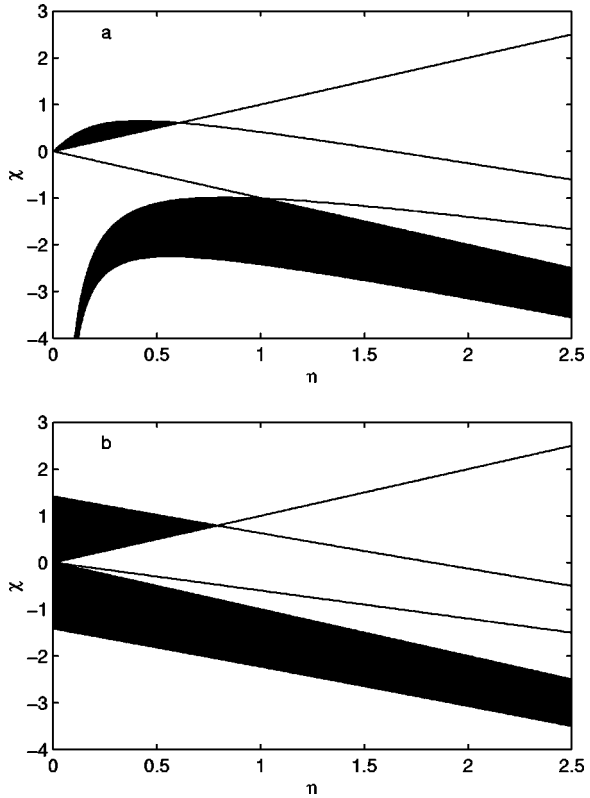

FIG. 1. (a) Parameter regions (χ vs η) for solitons' existence (dark areas). $a_1=0.2$, $n_0=3.5$, $\omega_0/\omega_c-1=-0.03$. The solid lines are the roots of Eq. (28) and $\chi=-\eta$. (b) The same as (a), but the LFC is neglected, i.e., $\epsilon=0$.

$\eta>0.608$, only one frequency band remains for solitons. Compared with Fig. 1(b), where LFC is not included, the NDD interaction has little effects if the TLS density is very low ($\eta\gg1$). However, if the TLS density is not very low, $\eta<1$, the NDD interaction significantly modifies the region where gap solitons exist. The upper band in Fig. 1(a) is much smaller than the upper band in Fig. 1(b). Especially, when $0.608<\eta<0.791$, the upper band will exist in Fig. 1(b) but disappear in Fig. 1(a). For moderate η, the lower bands in Figs. 1(a) and 1(b) are different but they still have some common region. If $\eta<0.278$, the dark areas in Figs. 1(a) and 1(b) will have no common region. When η is very small, gap solitons are filled in the frequency near the gap center in Fig. 1(b), while the inclusion of LFC leads to almost no gap solitons existing in the frequency near the gap center as shown in Fig. 1(a). Since small η corresponds to high TLS density, Fig. 1(a) shows that the gap solitons in RABR are difficult to be observable if the TLS density is high enough.

We have performed numerical studies with different parameters. We found that increasing the TLS frequency detuning can increase the frequency region of the gap solitons. An example is shown in Fig. 2(a), where only the detuning is changed compared with Fig. 1(a). On the other hand, increasing a_1 will enhance the NDD interaction, and decrease the frequency region of the gap solitons. In Fig. 2(b), $a_1=0.3$, $n_0=3.5$, $\omega_0/\omega_c-1=-0.03$, the dark areas are smaller than those shown in Fig. 1(a).

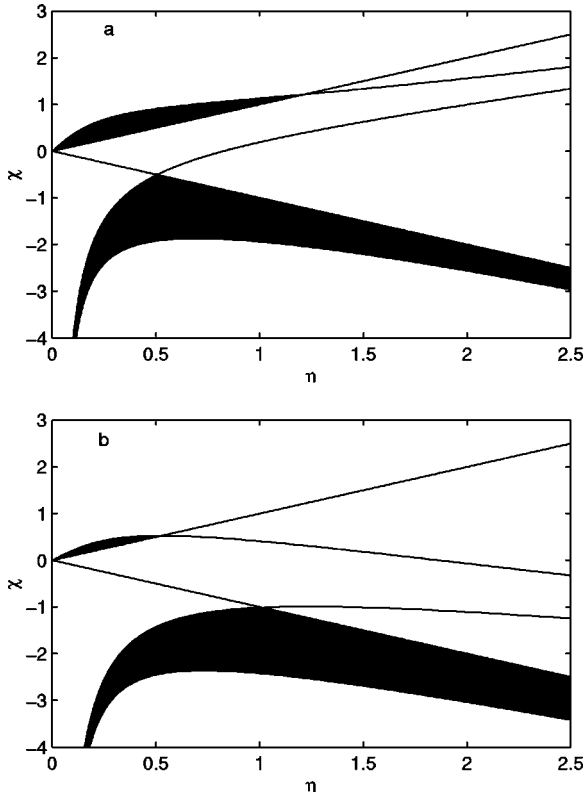

FIG. 2. (a) Parameter regions (χ vs η) for solitons' existence (dark areas). $a_1=0.2$, $n_0=3.5$, $\omega_0/\omega_c-1=0.03$. The solid lines are the roots of Eq. (28) and $\chi=-\eta$. (b) $a_1=0.3$, $n_0=3.5$, $\omega_0/\omega_c-1=-0.03$.

III. NUMERICAL SIMULATION

To study the evolution and stability of these standing solitons, we use numerical methods to solve the coupling Eqs. (8)–(11) directly. In the presented numerical results, we set $a_1=0.2$, $n_0=3.5$, $\omega_0/\omega_c-1=-0.03$. The initial condition takes the form $\Sigma_+(\zeta,0)=s(\zeta)+n(\zeta)$ with the small random noise $n(\zeta)$.

In the first example, we select $\chi=0.5029$, $\eta=0.3571$ which is in the upper frequency band in Fig. 1(a). The evolution shown in Fig. 3 indicates that this soliton is not stable. The other simulation with different χ, η in the upper frequency band also leads to an unstable evolution.

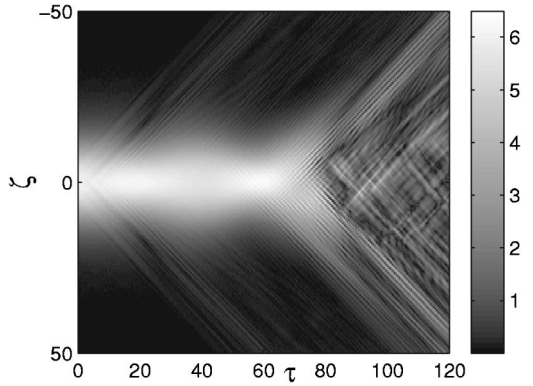

FIG. 3. Evolution of $|\Sigma_+|$ with additive noise, $\chi=0.2982$, $\eta=0.2131$.

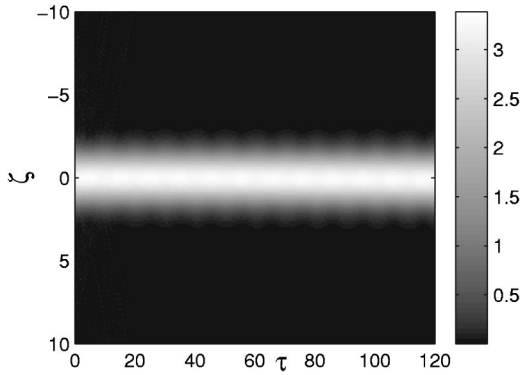

FIG. 4. Evolution of $|\Sigma_+|$ with random noise, $\chi=-1.5$, $\eta=0.5$.

On the other hand, for those χ, η in lower frequency band, the corresponding solitons seem stable during the simulation time. In Fig. 4, $\chi=-1.5$, $\eta=0.5$, the standing soliton retains the initial shape but there are small amplitude oscillations. Another example is for $\chi=-2.4649$, $\eta=0.2304$, under these parameters, standing soliton cannot exist in the original RABR model without LFC, but as shown in Fig. 5, there exist solitons and the solitons are stable in our model due to the inclusion of the NDD interaction.

Moving solitons can be also obtained with the procedure used in Ref. [9]: simulating Eqs. (8), (10), and (11) with an initial configuration in the form of the standing soliton multiplied by $\exp(ip\zeta)$ with a real p. An example is shown in Fig. 6.

Simulations with other values of a_1, n_0, and ω_0/ω_c were also performed. The results strongly suggest that the gap solitons in upper frequency band are more sensitive to noise than these gap solitons in lower frequency band.

In Refs. [3,10], the authors have discussed several experimental possibilities to realize the gap solitons in RABR. For example, quantum wells embedded in a semiconductor structure are considered with parameters $n_0\approx 3.6$, $\omega_c\approx 2.26\times 10^{15}\ \mathrm{s}^{-1}$, $\sigma\approx 10^{15}$–$10^{16}\ \mathrm{cm}^{-3}$, $a_1\approx 0.3$, and η vary from 0 to 10^2. Due to the NDD interaction, the gap solitons may not be observable if they are searched in the parameter regions predicted by the model without LFC when η is small (i.e., high density) as our results have shown.

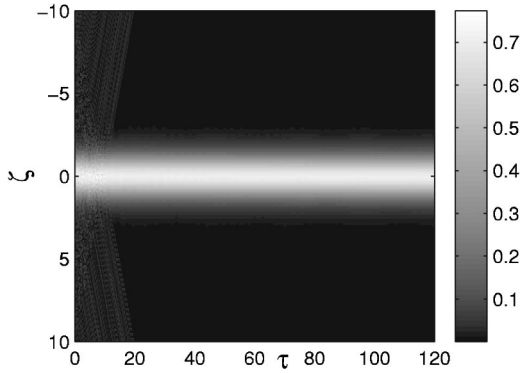

FIG. 5. Evolution of $|\Sigma_+|$ with random noise, $\chi=-2.4649$, $\eta=0.2304$.

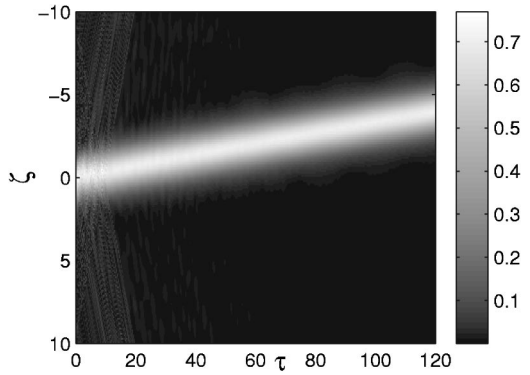

FIG. 6. Evolution of moving soliton $|\Sigma_+|$, $\chi=-2.4649$, $\eta=0.2304$. Initial profile is the standing soliton multiplied by $\exp(ip\zeta)$, $p=0.4$. Random noise is included.

IV. CONCLUSION

In conclusion, we have generalized the RABR model to include the NDD interaction. We find that the LFC significantly modifies the existence of the gap solitons. The upper frequency band of gap solitons in the RABR model with LFC is smaller than the upper frequency band of gap solitons in the RABR model without LFC, while the lower frequency band may be totally different from that with a low TLS density. Increasing the refractive-index modulation will enhance the NDD interaction. Numerical simulation suggests that these gap solitons in the upper frequency band may be unstable, but gap solitons in the lower frequency band are stable. Our results indicate that the NDD interaction cannot be neglected in the study of gap solitons in the RABR model.

ACKNOWLEDGMENTS

The support of the project by the National Key Basic Research Special Foundation (NKBRSF) under Grant No. G1999075200 and the Chinese National Natural Science Foundation (Grant No. 29673058) is acknowledged.

[1] J.P. Dowling, *Photonic and Sonic Band-Gap Bibliography*, URL http://home.earthlink.net/ jpdowling/pbgbib.html.
[2] C.M. de Sterke and J.E. Sipe, Prog. Opt. **33**, 203 (1994).
[3] G. Kurizki, A.E. Kozhekin, T. Opatrny, and B. Malomed, Prog. Opt. **42**, 93 (2001).
[4] W. Chen and D.L. Mills, Phys. Rev. Lett. **58**, 160 (1987); A.B. Aceves and S. Wabnitz, Phys. Lett. A **141**, 37 (1989); D.N. Christodoulides and R.I. Joseph, Phys. Rev. Lett. **62**, 1746 (1989).
[5] H.G. Winful and V. Perlin, Phys. Rev. Lett. **84**, 3586 (2000).
[6] C. Conti, S. Trillo, and G. Assanto, Phys. Rev. Lett. **78**, 2341 (1997); H. He and P.D. Drummond, *ibid.* **78**, 4311 (1997); T. Peschel *et al.*, Phys. Rev. E **55**, 4730 (1997).
[7] B.J. Eggleton *et al.*, Phys. Rev. Lett. **76**, 1627 (1996); J. Opt. Soc. Am. B **16**, 587 (1999).
[8] A. Kozhekin and G. Kurizki, Phys. Rev. Lett. **74**, 5020 (1995).
[9] A.E. Kozhekin, G. Kurizki, and B.A. Malomed, Phys. Rev. Lett. **81**, 3647 (1998).
[10] T. Opatrny, B.A. Malomed, and G. Kurizki, Phys. Rev. E **60**, 6137 (1999).
[11] M. Blaauboer *et al.*, Phys. Rev. E **62**, R57 (2000); Phys. Rev. Lett. **84**, 1906 (2000).
[12] B.I. Mantsyzov, Opt. Commun. **189**, 275 (2001).
[13] C.M. Bowden and J.P. Dowling, Phys. Rev. A **47**, 1247 (1993).
[14] Y. Ben-Aryeh, C.M. Bowden, and J.C. Englund, Phys. Rev. A **34**, 3917 (1986); M.P. Hehlen *et al.*, Phys. Rev. Lett. **82**, 3050 (1999).
[15] M.G. Benedice *et al.*, Phys. Rev. A **43**, 3845 (1991).
[16] M.E. Crenshaw, M. Scalora, and C.M. Bowden, Phys. Rev. Lett. **68**, 911 (1992).
[17] J.P. Dowling and C.M. Bowden, Phys. Rev. Lett. **70**, 1421 (1993).
[18] N. Wang and H. Rabitz, Phys. Rev. A **51**, 5029 (1995).
[19] M.E. Crenshaw and C.M. Bowden, Phys. Rev. Lett. **85**, 1851 (2000).
[20] J.T. Mannassah and I. Cladkova, Opt. Commun. **196**, 221 (2001).
[21] A.A. Afanas'ev *et al.*, J. Opt. Soc. Am. B **19**, 911 (2002).